Electronic Supplementary Material (ESI) for Journal of Materials Chemistry C.

Ultra-smooth and robust graphene-based hybrid anode for high-performance flexible organic light-emitting diodes

Zhikun Zhang,[a, b†] Lianlian Xia,[c†] Lizhao Liu,[d†] Yuwen Chen,[e] Zuozhi Wang,[a, b] Wei Wang,[a, b] Dongge Ma,[e*] and Zhaoping Liu[a, b*]

[a] *CAS Engineering Laboratory for Graphene, Ningbo Institute of Materials Technology and Engineering, Chinese Academy of Sciences, Zhejiang 315201, P. R. China*

[b] *Key Laboratory of Graphene Technologies and Applications of Zhejinag Province, CAS Engineering Laboratory for Graphene, Ningbo Institute of Materials Technology & Engineering, Chinese Academy of Sciences, Zhejiang 315201, P. R. China*

[c] *State Key Laboratory of Chemical Engineering, College of Chemical and Biological Engineering, Zhejiang University, Hangzhou 310027, P. R. China*

[d] *Key Laboratory of Materials Modification by Laser, Ion and Electron Beams (Ministry of Education), Dalian University of Technology, Dalian 116024, P. R. China*

[e] *Institute of Polymer Optoelectronic Materials and Devices, State Key Laboratory of Luminescent Materials and Devices, South China University of Technology, Guangzhou 510640, P. R. China*

[*] *Corresponding author. E-mail: liuzp@nimte.ac.cn (Zhaoping Liu)*

[*] *Corresponding author. E-mail: msdgma@scut.edu.cn (Dongge Ma)*

In order to eliminate the adverse effects of the rough surface, a series of PET substrates are treated by the selective etching solution with different concentrations at room temperature. In this work, the selective etching solutions are composed of H_2SO_4 and H_2O_2 with the volume ratio of H_2SO_4 : H_2O_2 varied from 1:9 to 9:1. Fig. S1 shows the typical images of PET substrates before and after treated by the selective etching solution at room temperature. As shown in Fig. S1b, it can be seen that though the PET substrates soaked in concentrated etching solution can be quickly hydrolyzed when added to water, the surface morphology and optical transparency of PET substrates are also severely destroyed. However, when the etching solution volume ratio of H_2SO_4:H_2O_2 is adjusted to be 7:3, the rough surface of PET substrate can be effectively smoothed at room temperature for 30~40 min, and no obvious damages can be found on the surface. But when the volume ratio of H_2SO_4:H_2O_2 is lower than 7:3, the etching time will be significantly extended because the hydrolysis speed of PET decreases with the dilution of H_2SO_4. Therefore, it can be concluded that the harsh H_2SO_4 treatment is incompatible with the flexible PET substrate, and the optimal volume ratio of the selective etching solution is finally determined to be 7:3.

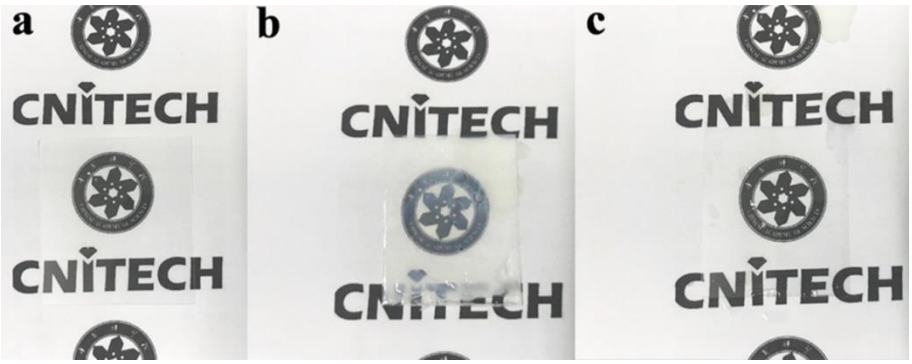

Fig. S1 Typical images of PET substrates before and after smoothing treatment by the selective etching solution with different volume ratio of H_2SO_4 : H_2O_2 at room temperature. (a) Untreated. (b) H_2SO_4 : H_2O_2 >7:3, (c) H_2SO_4 : H_2O_2≤7:3.

To validate our theoretical results and simultaneously explore the optimum thickness, in fact, direct and polymer-free manual transfer of CVD-grown graphene films with the number of layers from 1 to 4 are also carried out during our experiment process. As shown in Fig. S2a, it is very hard to realize intact and damage-free manual transfer of single-layer graphene film without relying on any supporting layer, but instead, it will breaks into pieces even under the condition of surface tension control of the etching solution. When the number of layers increases from 2 to 4 (As shown in Fig. S2b-f), though the multilayer graphene films can float calmly on the etchant solution, cracks are readily formed when we try to collect it on a PET substrate. However, when the number of layers increases up to 5 or more, the graphene films show significantly enhanced damage-tolerance behavior. The 5L-graphene films can float calmly on the etchant solution, and no obvious cracks can be observed during the transfer process. Considering that the optical transmittance of graphene films decreases with the increase of number of layers, 5L-graphene films are finally selected as the transparent conductive electrode (TCE) in this work. The graphene films used in this paper were grown by CVD on copper foils in a tri-zone tube furnace (BTF-1200C). Typically, a roll of 25 μm-thick copper foil (99.99 %) was cleaned by ethanol to remove the absorbents and organic contaminations before using. To avoid severe deformation of copper foil caused by thermal stress during rapid warming process, the copper foil was firstly heated to 400 ℃ in 30 min, then to 1000 ℃ in 60 min, and finally to 1035 ℃ in 10 min, under a mixture of H_2 (10 sccm) and Ar (100 sccm) in a 3-inch-wide tubular quartz reactor. Subsequently, a mixture of H_2 (100 sccm), and CH_4 (10 sccm), and Ar (100 sccm) is introduced into the chamber to initiate graphene growth. After 40 min of deposition, the CH_4 gas was shut off, followed by a slow cooling process to room temperature under the protection of a mixture of H_2 (10 sccm) and Ar (100 sccm). Note that the main difference of growth parameters of 1 to 4-layer CVD-grown graphene films is the cavity pressure (100 Pa, 800 Pa, 1500 Pa, 1.0 $\times 10^5$ Pa).

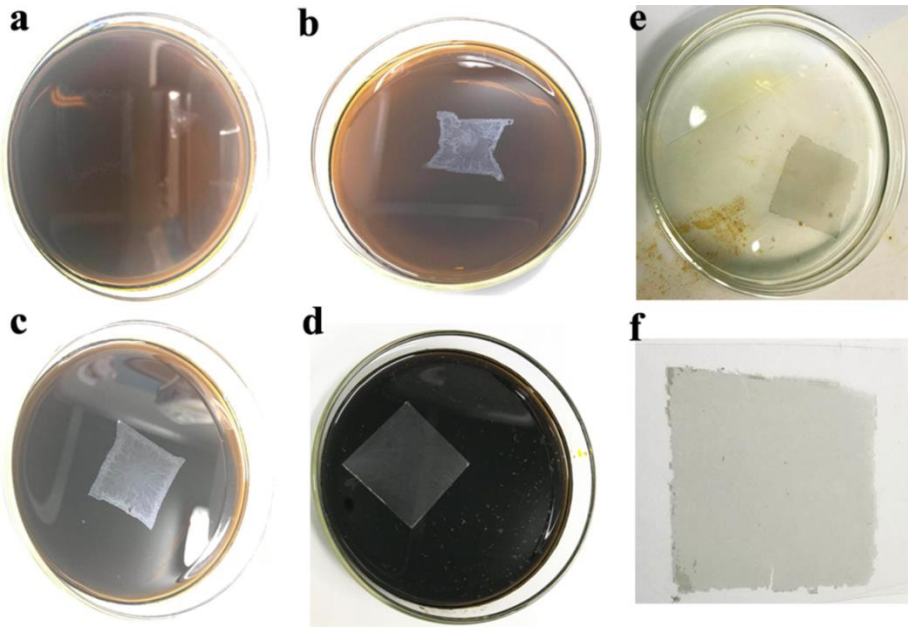

Fig. S2 Direct and polymer-free transfer of CVD-grown Graphene films with different numbers of layers. (a) 1-layer, (b) 2-layer, (c) 3-layer, (d) 4-layer graphene after removing the Cu foil by $FeCl_3$ etching, (e) A 4-layer graphene floating on deionized water for the removal of the residual $FeCl_3$ etching solution, (f) 4-layer graphene films on a PET substrate.

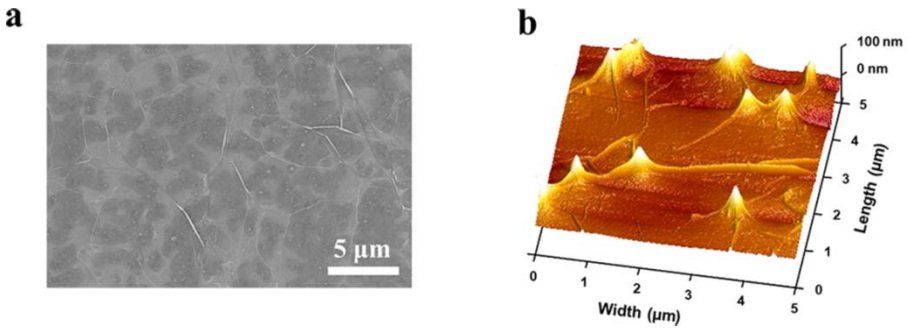

Fig. S3 Surface morphology and roughness of the transferred graphene films. (a) An SEM image of the CVD graphene after transferred onto the SiO_2/Si substrate, (b) AFM image of the surface morphology of a large area CVD-grown graphene film after transferred onto the pristine commercial PET substrate.

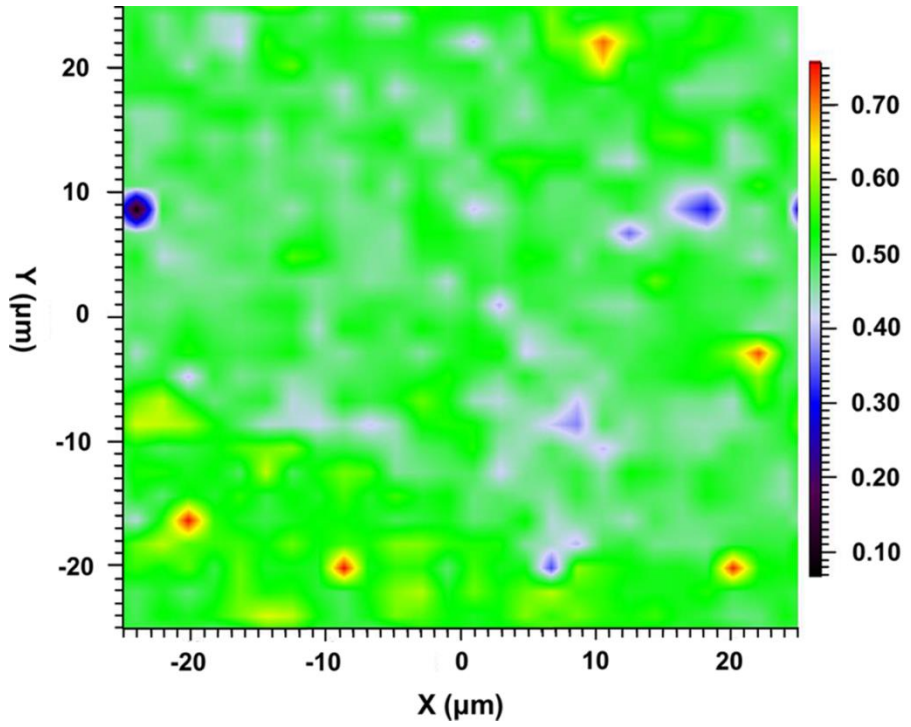

Fig. S4 The corresponding ID/IG ratio mapping image of the graphene film.

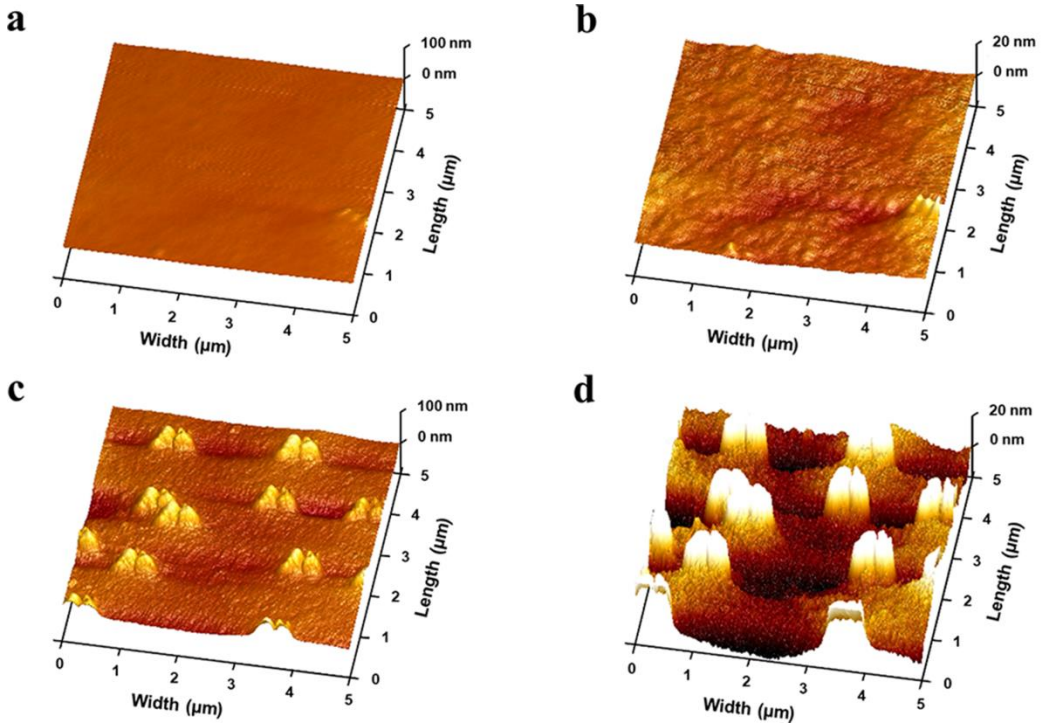

Fig. S5 Surface morphology and roughness of the graphene/PET anode. (a, b) AFM images of 5L-graphene/pristine PET substrate coated by a thin buffer layer of PEDOT:PSS film, (c, d) 5L-graphene/smoothed PET substrate after spin-coated by a thin buffer layer of PEDOT:PSS film. Note: the height of the exposed part of the spike is ~ 50 nm.

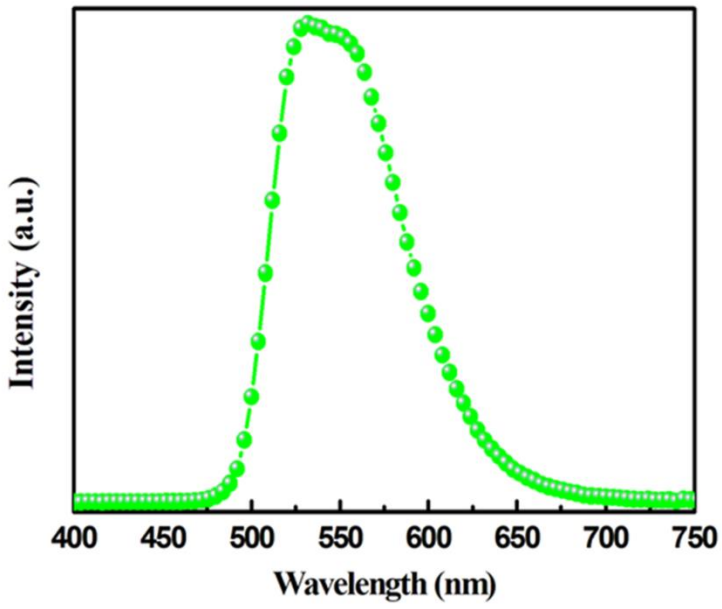

Fig. S6 Electroluminescence spectrum of our OLED.

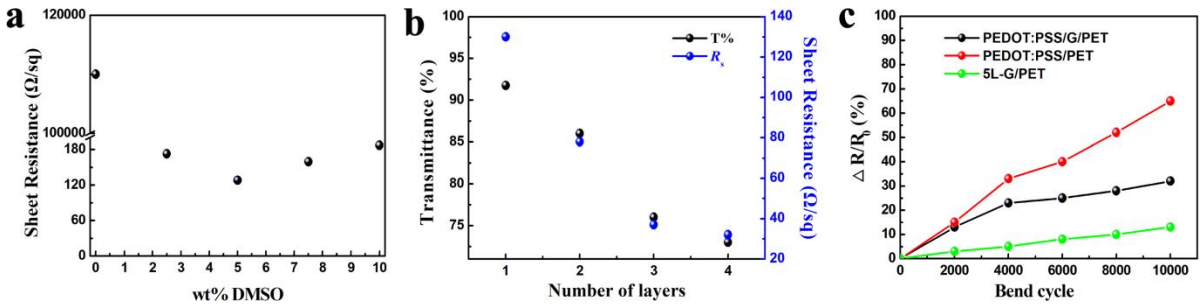

Fig. S7 (a) The R_s of the PEDOT:PSS films as a function of DMSO concentration, (b) Number of PEDOT:PSS layers in a film versus sheet resistance and transmittance at 550 nm, (c) Sheet resistance change of 5L-Graphene flims, PEDOT:PSS, and PEDOT:PSS/Graphene films on PET substrates as a function of number of bending cycles.

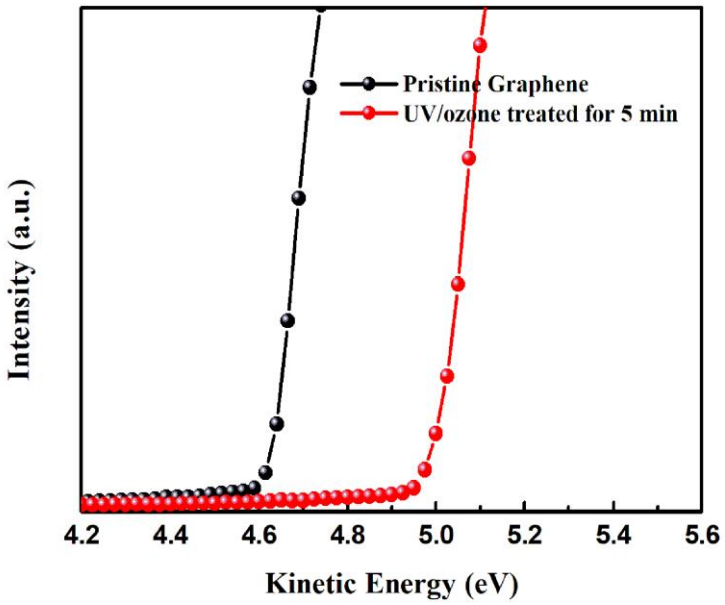

Fig. S8 The ultraviolet photoelectron spectroscopy (UPS) spectra of the pristine graphene and graphene oxide (GO)/graphene heterostructure on the SiO_2/Si substrates. The work functions of graphene and GO/G are measured to be ca. 4.6 and 5.0 eV, respectively.

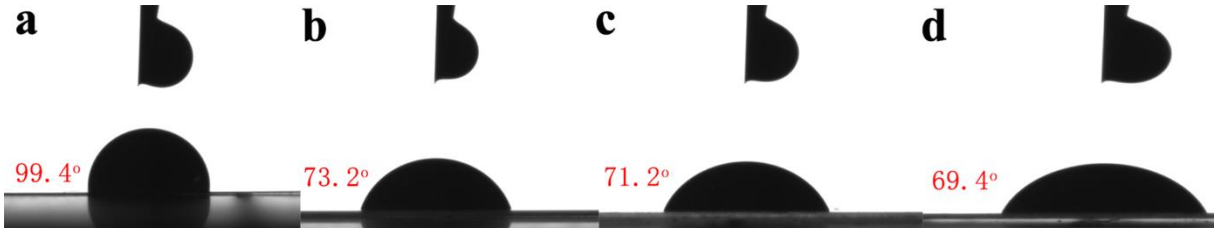

Fig. S9 The wettability characteristics of PEDOT:PSS (PH 1000) droplet on the graphene film before and after ozone treatment for different time. (a) Untreated graphene films, (b) 3 min, (c) 5 min, (d) 7 min.

Due to the hydrophobic nature of graphene films, hole injection layer (HIL) materials, such as poly(3,4-ethylenedioxythiophene)/poly(styrenesulfonate) (PEDOT:PSS) or 1, 4, 5, 8, 9, 11-Hexaazatriphenylenehexacarbonitrile (HATCN), are difficult to be uniformly deposited on the graphene surface, but instead, they will aggregate and tend to form irreversible agglomerates on the graphene surface. As shown in Fig. S9a, it can be seen obviously that the droplet of PEDOT:PSS shows a poor wettability with large contact angle (θ) of 99.4° on the pristine graphene surface. Therefore, mild UV/ozone treatments were carried out to improve the wetting properties of graphene film, which allows the easy deposition of HIL layers on the graphene surface. As shown in Fig. S9b-d, with the increase of UV/ozone treatment time from 3 to 7 min, the value of θ decreases from 73.2° to 69.4°, indicating the wetting properties of graphene film have been significantly improved. However, according to our previous work, the graphene film shows a sharp increase in the sheet resistance (R_s) after 5 min. To meet the electrical conductivity requirement of OLEDs, the optimal treatment time is therefore determined to be 5 min.

Table S1 Summary of device performance of typical OLEDs made with different graphene (G)-hybrid-TCEs in recent years.

Emission color	**Graphene-hybrid-TCEs**	**RMS/R_s /T@ 550nm/WF (nm/Ω sq^{-1}/%/eV)**	**Device structure**	**Max. CE ($cd\ A^{-1}$)**	**Max. PE ($lm\ W^{-1}$)**	**Active area (cm^2)**	**Refs.**
Green	SDBS-Graphene /PEDOT:PSS composite electrode	9.2/80±10/79/~5	PET/GCE/PEDOT:PSS/TPD/Alq_3/LiF/Al	3.9	-	~ 0.1	1
Green	Copper (Cu)/graphene composite anode	-/~0.0039/0/~4.46	Cu/graphene/V_2O_5/NPB/Alq_3/Alq_3:C545T/Bphen:Cs_2CO_3/Sm/Au	6.1	7.6	0.04	2
Yellow	CVD-graphene and PEDOT:PSS hybrid anode	-/~90/92.8/~4.9	Graphene sheet/PEDOT:PSS/PDY-132/ZnO/PEO/TBABF4/Al	0.89	-	0.06	3
Green	Monolayer graphene doped by TiO_x and PEDOT:PSS	0.976/~86/94.1/~5.12	G-TiO_x-PEDOT:PSS/NPB/Alq_3:C545T/Alq_3/LiF/Al	10.11 @ ~1000 cd m^{-2}	5.41 @ ~1000 cd m^{-2}	0.1	4
Green	Double-layered graphene/PEDOT:PSS	-/320/~80/-	Graphene/PEDOT:PSS/NPB/Alq_3/LiF/Al	1.09	-	0.16	5
Green	PEDOT:PSS and GO:SDBS hybrid anodes and 6 wt% dimethyl sulfoxide (DMSO)	1.32/85/87~5.1-5.2	PEN or Glass/ITO or hybrid anode/NPB/Alq_3/Bphen/Bphen:$CsCO_3$/Al	2.7	1.8	0.09	6
White	Double-layered graphene/PEDOT:PSS anode	5.26/300/~78/5.2	Graphene/PEDOT:PSS/NPB/CBP:Ir$(ppy)_3$:Rubrene/NPB/DPVBi/Bphen/Li	0.91	-	0.16	7

			F/Al				
Green	Graphene-on-Single walled carbon nanotube (SWCNTs) hybrid films	-/76/~89.13/~4.85	PBASE doped LBL stacking of FLG on CNT arrays/PEDOT:PSS with PFI/NPB/CBP:Ir(ppy)$_3$/BAlq$_3$/Alq$_3$/LiF/Al	~14.7	9.2	-	8
White	Graphene oxide (GO) soldered Silver Nanowire (AgNW) network	-/14/88/-	GO-AgNW/PUA/PEDOT:PSS/Emissive layer/PEI/GO-AgNW/PUA	4.0	-	0.12	9
Green	PEDOT:PSS:graphene:ethylcellulose (PEDOT:PSS:G:EC) hybrid cathode	0.87/13/78/-	PEDOT:PSS:G:EC/P-PPV/MoO$_x$/Ag	-	-	0.08	10
Green	PEDOT:PSS/GO composite anode	1.52/82.3/85/5.32	PEDOT:PSS/GO/NPB/Alq$_3$/LiF/Al	5.71	-	0.04	11
Green	HI-treated PEDOT:PSS:GO hybrid anode	1.507/92/91/4.82	PEDOT:PSS:GO/NPB/Alq$_3$/LiF/Al	~1.5	-	0.09	12
Green	CVD-graphene on Ag nanowire (NW) networks anode	-/30/86.9/-	p-Ag NW /Graphene/ PEDOT:PSS/ NPB/Alq$_3$/LiF/Al	1.8	0.6	-	13
Green	Graphene/AgNW/Polymer hybrid electrode	2.58/8.06/88.3/-	GN-A-P/MoO$_3$/NPB/Alq$_3$/LiF/Ag	2.11	-	0.16	14
Green	AgNWs/PEDOT:PSS/SLG (single-layer graphene) composite	6.4/30±5/87/-	AgNWs/PEDOT:PSS/SLG/NPB/Alq$_3$/LiF/Al	1.78	-	0.09	15

	anode						
Green	Single-layer Graphene/silver composite anode	2.09/8.5±0.5/74/4.9	Anode/MoO_3/TAPC/Alq_3:C545T/Alq_3/Liq/Al	-	-	-	16
Yellow	Silver nanowire and electrochemical exfoliated graphene (AgNWs-EG)	4.6/13.7/~80/-	AgNWs-EG/PEDOT:PSS/SY-PPV/Ba/Al	-	-	-	17
Green	SLG/AgNWs composite electrodes	1~3/27/86.7/5.1	SLG/AgNWs/Hat-cn/TAPC/C545T:Alq_3/Alq_3/Liq/Al	-	-	-	18
Green	PDA-RGO/SWCNT/PEDOT:PSS anode	2.41/52.2/88.7/-	PDA-RGO/SWCNT/PEDOT/NPB/Alq_3/LiF/Al	2.13	-	-	19
Yellow	Single-layer graphene/CNT/AZO/Au NP anode	-/~100/96/-	GCNT/AZO/Au NP/PEDOT:PSS/SY-PPV/LiF/Al	~2.1	-	-	20
Green	Silver nanowire/Graphene	6.4/26.4/91.5/-	AgNW/G/PEDOT:PSS/NPB:MoO_3/NPB/TCTA/MCP:Ir(ppy)$_3$/TPBi/Liq/Al	22.2	5.81	-	21
Green	**5L Graphene/PEDOT:PSS anode**	**0.439/80/83/~5.0**	**Graphene/PEDOT:PSS/HATCN/TAPC/Ir(ppy)$_2$(acac):Bepp2/Bepp2/LiF/Al**	**76 - 20**	**61 -**	**0.16**	**This work**

References

1 H. Chang, G. Wang, A. Yang, X. Tao, X. Liu, Y. Shen and Z. Zheng, *Adv. Funct. Mater.*, 2010, **20**, 2893-2902.

2 H. Meng, J. Luo, W. Wang, Z. Shi, Q. Niu, L. Dai and G. Qin, *Adv. Funct. Mater.*, 2013, **23**, 3324-3328.

3 S. Shin, J. Kim, Y.-H. Kim and S.-I. Kim, *Curr. Appl. Phys.,* 2013, **13**, S144-S147.

4 X.-Z. Zhu, Y.-Y. Han, Y. Liu, K.-Q. Ruan, M.-F. Xu, Z.-K. Wang, J.-S. Jie and L.-S. Liao, *Org. Electron.,* 2013, **14**, 3348-3354.

5 X. Wu, F. Li, W. Wu and T. Guo, *Vacuum,* 2014, **101,** 53-56.

6 X. Wu, J. Liu, D. Wu, Y. Zhao, X. Shi, J. Wang, S. Huang and G. He, *J. Mater. Chem. C,* 2014, **2,** 4044-4050.

7 X. Wu, F. Li, W. Wu, T. Guo, *Appl. Surf. Sci.,* 2014, **295**, 214-218.

8 Y. Liu, E. Jung, Y. Wang, Y. Zheng, E. J. Park, S. M. Cho and K. P. Loh, *Small,* 2014, **10**, 944-949.

9 J. Liang, L. Li, K. Tong, Z. Ren, W. Hu, X. Niu, Y. Chen and Q. Pei, *ACS nano,* 2014, **8**, 1590-1600.

10 X. Hu, L. Chen, T. Ji, Y. Zhang, A. Hu, F. Wu, G. Li and Y. Chen, *Adv. Mater. Interfaces,* 2015, **2**, 1500445.

11 Y.-F. Liu, J. Feng, Y.-F. Zhang, H.-F. Cui, D. Yin, Y.-G. Bi, J.-F. Song, Q.-D. Chen and H.-B. Sun, *Org. Electron.,* 2015, **26,** 81-85.

12 X. Wu, L. Lian, S. Yang and G. He, *J. Mater. Chem. C,* 2016, **4**, 8528-8534.

13 W. Zhou, J. Chen, J. Chen, C. Zheng, Z. Gao, B. Mi, H. Zhang and Y. Ma, *J. Nanosci. Nanotechno.,* 2016, **16**, 12609-12616.

14 H. Dong, Z. Wu, Y. Jiang, W. Liu, X. Li, B. Jiao, W. Abbas and X. Hou, *ACS Appl. Mater. Interfaces,* 2016, **8**, 31212-31221.

15 Y. Xu, X. Wei, C. Wang, J. Cao, Y. Chen, Z. Ma, Y. You, J. Wan, X. Fang and X. Chen, *Sci. Rep.,* 2017, **7**, 45392.

16 K. Li, H. Wang, H. Li, Y. Li, G. Jin, L. Gao, M. Marco and Y. Duan, *Nanotechnology,* 2017, **28**, 315201.

17 A. G. Ricciardulli, S. Yang, G. J. A. H. Wetzelaer, X. Feng and P. W. M. Blom, *Adv. Funct. Mater.,* 2018, **28**, 1706010.

18 H. Li, Y. Liu, A. Su, J. Wang and Y. Duan, *Sci. Rep.,* 2019, **9**, 17998.

19 T. Wang, L.-C. Jing, Q. Zhu, A. S. Ethiraj, Y. Tian, H. Zhao, X.-T. Yuan, J.-G. Wen, L.-K. Li and H.-Z. Geng, *Appl. Surf. Sci.,* 2019, **500**, 143997.

20 P. Kumar, K. L. Woon, W. S. Wong, M. S. M. Saheed and Z. A. Burhanudin, *Synthetic Met.,* 2019, **257**, 116186.

21 J. Zhang, Y. Li, B. Wang, H. Hu, B. Wei and L. Yang, *Micromachines,* 2019, **10**, 517.